NHE3 in an ancestral vertebrate: primary sequence, distribution, localization, and function in gills

Keith P. Choe, Akira Kato, Shigehisa Hirose, Consuelo Plata, Aleksandra Sindic, Michael F. Romero, J. B. Claiborne and David H. Evans

Am J Physiol Regul Integr Comp Physiol 289:1520-1534, 2005. First published Jun 30, 2005;
doi:10.1152/ajpregu.00048.2005

Am J Physiol Regul Integr Comp Physiol 289: R1520–R1534, 2005.
First published June 30, 2005; doi:10.1152/ajpregu.00048.2005.

NHE3 in an ancestral vertebrate: primary sequence, distribution, localization, and function in gills

Keith P. Choe,[1] Akira Kato,[2] Shigehisa Hirose,[2] Consuelo Plata,[3] Aleksandra Sindić,[3] Michael F. Romero,[3] J. B. Claiborne,[4] and David H. Evans[1]

[1]*Department of Zoology, University of Florida, Gainesville, Florida;* [2]*Department of Biological Sciences, Tokyo Institute of Technology, Yokohama, Japan;* [3]*Department of Physiology and Biophysics and Department of Pharmacology, Case Western Reserve University, Cleveland, Ohio; and* [4]*Department of Biology, Georgia Southern University, Statesboro, Georgia*

Submitted 24 January 2005; accepted in final form 27 June 2005

Choe, Keith P., Akira Kato, Shigehisa Hirose, Consuelo Plata, Aleksandra Sindić, Michael F. Romero, J. B. Claiborne, and David H. Evans. NHE3 in an ancestral vertebrate: primary sequence, distribution, localization, and function in gills. *Am J Physiol Regul Integr Comp Physiol* 289: R1520–R1534, 2005. First published June 30, 2005; doi:10.1152/ajpregu.00048.2005.—In mammals, the Na^+/H^+ exchanger 3 (NHE3) is expressed with Na^+/K^+-ATPase in renal proximal tubules, where it secretes H^+ and absorbs Na^+ to maintain blood pH and volume. In elasmobranchs (sharks, skates, and stingrays), the gills are the dominant site of pH and osmoregulation. This study was conducted to determine whether epithelial NHE homologs exist in elasmobranchs and, if so, to localize their expression in gills and determine whether their expression is altered by environmental salinity or hypercapnia. Degenerate primers and RT-PCR were used to deduce partial sequences of mammalian NHE2 and NHE3 homologs from the gills of the euryhaline Atlantic stingray (*Dasyatis sabina*). Real-time PCR was then used to demonstrate that mRNA expression of the NHE3 homolog increased when stingrays were transferred to low salinities but not during hypercapnia. Expression of the NHE2 homolog did not change with either treatment. Rapid amplification of cDNA was then used to deduce the complete sequence of a putative NHE3. The 2,744-base pair cDNA includes a coding region for a 2,511-amino acid protein that is 70% identical to human NHE3 (SLC9A3). Antisera generated against the carboxyl tail of the putative stingray NHE3 labeled the apical membranes of Na^+/K^+-ATPase-rich epithelial cells, and acclimation to freshwater caused a redistribution of labeling in the gills. This study provides the first NHE3 cloned from an elasmobranch and is the first to demonstrate an increase in gill NHE3 expression during acclimation to low salinities, suggesting that NHE3 can absorb Na^+ from ion-poor environments.

osmoregulation; sodium/hydrogen exchanger; sodium/potassium adenosinetriphosphatase; elasmobranch

IN MAMMALIAN CELLS, Na^+/H^+ exchangers (NHEs) or antiporters catalyze 1:1 electroneutral exchange of Na^+ and H^+ down their respective concentration gradients (28, 41, 46, 47, 64, 73). The first NHE was cloned from mouse cells (NHE1) (56), and it was followed by NHE3 (48, 61) and NHE2 (18, 62) from rat and rabbit intestines. Nine isoforms have now been identified in the human genome (SLC9A1–9) that have diverse tissue, cell, and membrane localizations (8, 46). NHE2 and NHE3 are expressed in the apical membranes of gastrointestinal and renal cells, where they can participate in systemic Na^+ absorption and H^+ secretion. In the kidney, NHE2 is found in the cortical thick ascending limb, macula densa, distal convoluted tubules, and connecting tubules (10), and NHE3 is found predominantly in the proximal convoluted tubule and to a lesser extent in the thick ascending limb (2, 5, 6). In renal proximal tubules of mammals, apical NHE3 is functionally linked to basolateral Na^+/K^+-ATPase and Na^+/HCO_3^- cotransporter in a mechanism that is responsible for the majority of Na^+ and HCO_3^- reabsorption in the kidney (63, 65), and NHE3 null mice have markedly decreased renal HCO_3^- and fluid absorption, systemic acidosis, hypotension, and elevated plasma aldosterone (36, 70). The function of NHE2 in the kidney is not yet clear, and NHE2 null mice have no measurable phenotypes that suggest renal absorptive malfunction (36).

In elasmobranchs, the gills are responsible for most of systemic Na^+ absorption and H^+ secretion instead of the kidneys (11, 15, 25). Fittingly, similarities between epithelial cells in the gills of an elasmobranch, Atlantic stingray (*Dasyatis sabina*), and renal tubule cells of mammals have been discovered. For example, apical immunoreactivity for a Cl^-/HCO_3^- exchanger (pendrin) and basolateral immunoreactivity for vacuolar H^+-ATPase occur in one cell type of stingray gills similar to type B intercalated cells of mammalian kidneys (25, 53). High levels of basolateral Na^+/K^+-ATPase immunoreactivity were observed in another gill cell type (50) that was hypothesized as the location of transepithelial Na^+ absorption, and in vivo flux studies demonstrated a link between Na^+ and H^+ (23, 24). However, an apical mechanism of Na^+ and H^+ transport has not been identified, and no molecular sequence data exist for an NHE3 from an elasmobranch.

The gills of elasmobranchs provide a unique opportunity to study the roles of transporters in branchial Na^+ absorption and acid secretion without having to consider any potential dual functions in Na^+ and/or Cl^- secretion. Unlike teleosts (the largest group of fishes), elasmobranchs have an accessory organ that is responsible for NaCl secretion in seawater (i.e., rectal gland), and their gills do not appear to be involved in salt secretion (26, 66). However, few studies have been able to take advantage of this segregation of transport functions because most elasmobranchs are large (i.e., difficult to maintain) and euryhaline species are rare (only 3% of elasmobranch species live in both seawater and freshwater) (25). The Atlantic stingray is the only North American species of elasmobranch that has permanent populations in both seawater and freshwater (7, 31, 52). It is a small elasmobranch species (adults 300–800 g) that can be

Address for reprint requests and other correspondence: K. P. Choe, Anesthesiology Research Div., Vanderbilt Univ. Medical Center, T-4202 Medical Center North, 1161 21st Ave. South, Nashville, TN 37232-2520 (e-mail: keith.p.choe@vanderbilt.edu).

The costs of publication of this article were defrayed in part by the payment of page charges. The article must therefore be hereby marked "*advertisement*" in accordance with 18 U.S.C. Section 1734 solely to indicate this fact.

maintained in either fresh or seawater aquaria and therefore is well suited as a model for gill ion absorption (52).

The previously known link between Na^+ and H^+ transport and the demonstration of Na^+/K^+-ATPase-rich cells in elasmobranch gills led us to hypothesize that an apical NHE may be expressed in the gills of elasmobranchs, where it may function in systemic Na^+ absorption and H^+ secretion. Therefore, the first goals of this study were to determine whether NHE2 and/or NHE3 homologs exist in the gills of the Atlantic stingray and, if so, to determine whether mRNA expression of either was altered by acclimation to freshwater or hypercapnic acidosis. Furthermore, if expression for an NHE was elevated, we also sought to localize its expression in the gills relative to Na^+/K^+-ATPase and vacuolar H^+-ATPase. In this article, we report the first complete cDNA sequence for an NHE3 ortholog in an elasmobranch, demonstrate that NHE3 protein is located on the apical side of Na^+/K^+-ATPase cells, and report the first increase in gill NHE3 expression during acclimation to low salinities.

MATERIALS AND METHODS

Animals and standard holding conditions. All procedures were approved by the University of Florida Institutional Animal Care and Use Committee. Atlantic stingrays (*D. sabina*, ~154–658 g) were captured from waters surrounding Sea Horse Key, FL, in the Gulf of Mexico by using a cast net. They were transported to the University of Florida in Gainesville, FL, where they were held in a 380-liter tank containing 100% seawater from the Atlantic Ocean. The water pH was maintained between 7.8 and 8.2 with a commercial aquarium carbonate buffer (Seachem, Stone Mountain, GA), NH_3 and NO_3^- were maintained below 1 part per million with a biological filter, and temperature was maintained between 22 and 26°C. The room that housed the stingrays was on a 12:12-h light-dark cycle.

RT-PCR, cloning, and sequencing. Stingrays were anesthetized by an initial immersion in 150 mg/l MS-222 diluted in aquarium water. The anesthetic was diluted to 75 mg/l by addition of more water, and stingrays were perfused through the conus arteriosus with cold (~4°C) elasmobranch phosphate-buffered saline (10 mmol/l PBS was adjusted with NaCl, urea, and trimethylamine oxide to approximate the total osmolarity of stingray plasma) (52). The stingrays were then pithed, and gill filaments were removed with sterile, RNase-free tools and frozen in liquid nitrogen. Total RNA was then isolated with TRI reagent (Sigma, St. Louis, MO), and first-strand cDNA was synthesized from 2 μg of total RNA with a SuperScript II reverse transcriptase kit (Invitrogen, Carlsbad, CA), using oligo(dT) as a primer.

Degenerate primer pairs were then designed to amplify conserved regions of vertebrate ribosomal protein L8, NHE, and Na^+/K^+-ATPase proteins (Table 1). Each PCR was performed on one-twentieth of a reverse transcriptase reaction with a FastStart *Taq* DNA polymerase kit (Roche Applied Science, Indianapolis, IN) in a PCR Express thermocycler (ThermoHybaid, Franklin, MA) with standard cycling parameters. PCR products were visualized by ethidium bromide staining in 1.0–1.5% agarose gels, ligated into pCR 4-TOPO vectors, and transformed into TOP10 chemically competent cells by using a TOPO TA cloning kit for sequencing (Invitrogen). Plasmid DNA was then sequenced in both directions at the Marine DNA Sequencing Facility at the Mount Desert Island Biological Laboratory (Salisbury Cove, ME).

After the sequencing of initial fragments with degenerate primers, more of the cDNA for NHE3 was cloned and sequenced by primer walking with degenerate primers. Primers 5′ NHE3 CHF1 and DS R986 were used to extend toward the 5′ end, and primers DS F1414 and 3′ NHE3 CHR3 were used to extend toward the 3′ end (Table 1). Finally, 5′ and 3′ rapid amplification of cDNA ends (RACE) was used to finish the sequence. Briefly, 5′ and 3′ RACE cDNA were prepared with a GeneRacer kit (Invitrogen) according to the manufacturer's protocols. PCRs for 5′ RACE were completed with antisense primer 5′ RI and a sense primer that is included in the kit, and PCRs for 3′ RACE were completed with sense primers 3′ b F1 and 3′ b F2 and antisense primers that are included in the kit (Table 1). PCR, cloning, and sequencing were performed as described above, except for the use of touchdown cycle parameters and nested PCR to increase specificity. After the 5′ and 3′ ends of the NHE3 transcript were sequenced, specific primers were designed 15 bases upstream from the likely start

Table 1. *Primers used in PCR*

Name	Orientation	Nucleotide Sequence (5′ to 3′)
L8 F1 deg*	Sense	GGA TAC ATC AAG GGA ATC GTG AAR GAY ATH AT
L8 R1 deg*	Antisense	CCG AAA GGG TGC TCC CAN GGR TTC AT
L8 F1†	Sense	AAG AAG GCT CAG TTG AAC ATT GGA
L8 R2†	Antisense	TGT ACT TGT GAT AAG CCC GAC CAG
NHE F2 deg*	Sense	GCN GTK MTN GCN GTN TTY GAR GA
NHE R1 deg*	Antisense	GCN CCN CKN ARN CCN CCR TA
NHE2 F1†	Sense	ATA TCT TTG CTG GCA TTG CTC A
NHE2 R1†	Antisense	TGC GGG TAA CCA ATA GT
NHE3 F1†	Sense	GGT GTC ATC TTT GCA TTC C
NHE3 R1†	Antisense	CAC CAC CTG ATC TAT GAT CTC C
5′ NHE3 CHF1*	Sense	TTC AAA TTG TGA CTT GGA AAT GGS MNC AYG T
5′ DS R986	Antisense	TTC CAC CCA AAC TTA CAA CGA AGA
3′ DS F1414	Sense	CGT GTG GTG CAG TTG GAG ATC ATA
3′ NHE3 CHR3*	Antisense	CGT TTT CGC ATA GTC CGG TGR AAD ATY TC
5′ R1	Antisense	ACC TCT TCA AAC ACA GCC AAT ACA G
3′ b F2	Sense	ATA GCC GCC ATA AAC TAA TGC
3′ b F1	Sense	ACT CAT CTG TCT CTG CGG TGC T
NHE3 ORF F2	Sense	CGC GCA CAT AGA GCA C
NHE3 ORF R2	Antisense	TAA TGG AAA CCC GTG AAG TTC
NK2-F1 deg*	Sense	ATH GAR CAY TTY GTN CAY AT
P-R1 deg*	Antisense	TCN GGN GCN CCY TTC AT
NKA1 F1†	Sense	CTC TCA CTC ATC TTG GGA TAC AG
NKA1 R1†	Antisense	GGC ATC TCC AGC AAC ACT T

*Degenerate primer. †Real-time PCR primer.

codon and 44 bases after the likely stop codon to verify alignment of the complete cDNA (Table 1). PCR was performed on gill cDNA with primers NHE3 ORF F2 and NHE3 ORF R2, using the hot start version of TaKaRa ExTaq (Takara Bio, Shiga, Japan). The resulting product was cloned and sequenced as described above with sequencing primers spaced apart by ~600 bases.

Multiple-tissue relative quantitative PCR. To determine whether other acid-base and/or ion transport tissues express the putative transporter mRNAs, we performed relative quantitative RT-PCR on total RNA from gill, stomach, kidney, spiral value intestine, and rectal gland as described previously (14). Briefly, cDNA was produced from the tissues of a seawater stingray as described above, but random primers were used so that ribosomal and messenger RNA would be reverse transcribed. Nondegenerate primer pairs (Table 1) were designed for each putative transporter sequence with OLIGO 6.7 (Cascade, CO) to amplify products with high efficiency (e.g., high melting temperature). To minimize the chance of amplifying contaminating genomic DNA, we designed primer pairs to include an intron-exon boundary that is conserved between vertebrate homologs (19, 32, 45). The specificities of all primer pairs used for tissue distribution were verified by sequencing PCR products. A QuantumRNA 18S internal standard primer kit (Ambion, Austin, TX) was used to control for variability in RNA quality and quantity between the different tissues tested. Multiplex PCR with primers for 18S and each putative transporter were then optimized to ensure that the reactions were terminated during the exponential phase and that the kinetics of 18S amplification approximated those of the putative transporter transcripts. Finally, the products were visualized by ethidium bromide staining in 1.5% agarose gels and photographed with Polaroid 667 film.

Sequence analysis. Sequence results for each initial degenerate primer pair were assembled, and the resulting contig amino acid translations were analyzed with the basic local alignment search tool (BLAST) on the National Center for Biotechnology Information website (http://www.ncbi.nlm.nih.gov/). NHE3 fragment sequences were assembled with GeneTools software (BioTools, Edmonton, AB, Canada), and the assembled nucleotide sequence was searched for open reading frames. The predicted amino acid sequence was aligned with other full-length vertebrate NHE3 proteins using PepTools software (BioTools). The expected locations of membrane-spanning regions and regions important for regulation of the transporter were taken from previously published reports (1, 37, 41, 72, 74). MEGA software (34) was used to make an unrooted phylogenetic tree of vertebrate NHE isoforms 1–5 with the neighbor-joining method and Poisson-corrected evolutionary distances (42). Branches were then tested for statistical significance by bootstrapping with 1,000 replicates. NHE sequences from *Fugu*, *Danio*, and *Tetraodon* (green pufferfish) were derived from genome databases.

Salinity transfer. Some of the tissues used for the salinity comparisons were taken from animals treated in a previous study (14). Briefly, eight stingrays were captured from Sea Horse Key and held in 100% seawater as described in *Animals and standard holding conditions*, except they were not fed. The stingrays were then divided into two groups: one group remained in 100% seawater (approximate concentrations in mmol/l: 517.36 Na^+, 8.66 Ca^{2+}, 11.54 K^+, 485.60 Cl^-), and the other was transferred to a separate 380-liter tank where they were gradually exposed to freshwater (buffered Gainesville tap water, approximate concentrations in mmol/l: 3.50 Na^+, 1.16 Ca^{2+}, 0.03 K^+, 0.40 Cl^-) (1 day in 75% seawater, 2 days in 50% seawater, and 1 day in 25% seawater) (11). Commercial carbonate buffers (Seachem Laboratories) were added to make the pH and HCO_3^- concentration stable and approximately equal in the two salinities (11). Stingrays remained in either seawater or freshwater for 1 wk, and total RNA was isolated for quantitative real-time PCR analysis as described above. Gill tissue was also fixed (3% paraformaldehyde, 0.05% glutaraldehyde, 0.05% picric acid in 10 mmol/l PBS, pH 7.3) for 24 h at 4°C for immunohistochemical analysis or snap frozen in liquid nitrogen for Western blot analysis. In addition, the gills from two stingrays that were previously collected from freshwater (Lake George, FL) and held in freshwater (*RT-PCR, cloning, and sequencing*) were fixed for immunohistochemical analysis. However, RNA was not available from these stingrays, and they were not analyzed for mRNA expression levels. The three salinity treatment groups are referred to as seawater (from Sea Horse Key), freshwater-acclimated (from Sea Horse Key but held in freshwater for 1 wk), and freshwater stingrays (from Lake George).

Exposure to hypercapnia. Tissues used for the hypercapnia comparisons were also taken from animals treated in a previous study (13). Briefly, 20 stingrays were captured and held in 100% seawater as indicated in *Animals and standard holding conditions*, except they were never fed. These stingrays were then exposed to normocapnic (air) or hypercapnic (1% CO_2 in air) water, as described previously (11). Stingrays were transferred into a 10.5-liter closed-recirculating chamber (1 per chamber) fitted with a countercurrent gas/water exchange column. All stingrays were first exposed to a pretreatment period of 4–5 h, when the exchange column received air from a gas mixer. After this pretreatment period, the exchange column received air (control) or 1% CO_2-99% air (hypercapnia). Total RNA was then isolated from the gills of stingrays after 2 or 4 h for quantitative real-time PCR as described in *RT-PCR, cloning, and sequencing*.

Quantitative real-time PCR. To measure relative expression levels, polyA RNA was reverse transcribed as described in *RT-PCR, cloning, and sequencing*, and the resulting cDNA was subjected to PCR in the presence of SYBR green (Molecular Probes, Eugene, OR) binding dye in a real-time thermal cycler (9). The primers used for tissue distribution were also used for quantitative real-time PCR (qRT-PCR) (Table 1), and qRT-PCR with gill RNA samples that were not reverse transcribed verified that no products were amplified from contaminating genomic DNA. All qRT-PCR reactions were run in triplicate and included 0.2 μl of cDNA (2.0 μl of a 1:10 dilution of original cDNA), 7.4 pmol of each primer, and SYBR green Master Mix (Applied Biosystems, Foster City, CA) in a total volume of 25 μl. All qRT-PCR reactions were run in an ABI 5700 sequence detection thermal cycler (Applied Biosystems) with the following cycling parameters: initial denaturing for 10 min at 95°C, followed by 40 cycles of 35 s at 95°C, 30 s at 60°C, and 30 s at 72°C. The final cycle was followed by a melting curve analysis to verify the amplification of a single product in each well. Specificities of all primer pairs were also verified by sequencing PCR products.

Relative gene expression was calculated from relative standard curves that used 10-fold serial dilutions of purified plasmid DNA as the template, and all results were normalized to ribosomal protein L8, a highly conserved gene for which expression in the gills remains constant during salinity and acid-base changes (unpublished observation). Unpaired Student's *t*-tests were used to compare seawater to freshwater-acclimated and control to hypercapnic expression levels. In addition, regression analysis of all relative expression data from 14 seawater control gill samples was conducted between all combinations of putative transporters to determine whether the expression of any transcripts was highly correlated. Alpha was set at 0.05 for all statistical tests.

In situ hybridization. Two constructs were made from the complete stingray NHE3 plasmid, one that included 30 bases of the 5′ untranslated region and the first 588 bases of the open reading frame (*Eco*R1 fragment, *probe 19*), and one that included the last 229 bases of the open reading frame and 65 bases of the 3′ untranslated region (*Hin*dIII/*Spe*1 fragment, *probe 1*). These fragments were gel purified and ligated into the corresponding cloning sites of pBluescript SK vectors (Stratagene, La Jolla, CA). Digoxigenin (DIG)-labeled sense and antisense RNA probes were then transcribed from T7 and T3 priming sites with DIG RNA labeling mix (Roche Applied Science). Gill sections from one of the seawater control stingrays were produced with the same methods used for immunohistochemical analysis, and RNA probes were allowed to anneal to native RNA in the

sections. Alkaline phosphatase-conjugated anti-DIG antibody and its substrates (nitro blue tetrazolium/5-bromo-4-chloro-3-indolylphosphate) were used to visualize the signal, followed by counterstaining with Kernechtrot (Muto Pure Chemicals, Tokyo, Japan). Some sections, serial to those stained with riboprobes, were labeled with an antibody that recognizes Na^+/K^+-ATPase, as described below.

Antibody production. A 636-bp fragment encoding the final 212 amino acids of the carboxyl tail of the putative NHE3 was subcloned into the *Bam*HI/*Eco*R1 sites of a pHAT10 bacterial expression vector (BD Biosciences, San Jose, CA), and the construct was transformed into *Escherichia coli* BL21 (codon plus). The resulting recombinant cells were grown at 27°C until the culture had an optical density of 0.7 at 600 nm. Isopropyl-β-D-thiogalactopyranoside was then added to a final concentration of 1 mmol/l, and incubation was continued for an additional 6 h. Cells were harvested from 4 liters of culture by centrifugation, resuspended in 150 ml of PBS containing 0.75 μg/ml lysozyme, disrupted by freeze-thaw and sonication, and centrifuged at 10,000 *g* for 30 min. The recombinant protein was purified from supernatant with BD TALON metal affinity resin (BD Biosciences) and dialyzed against PBS at 4°C. Polyclonal antibodies were prepared in four Wistar-Kyoto rats by first injecting 200 μg of protein in Freund's complete adjuvant near abdominal lymph nodes and intradermally. Two and three weeks after the initial injections, the rats were boosted intradermally with 200 μg of protein in Freund's incomplete adjuvant. Final bleeds were made 7 days after the third injection.

Immunohistochemistry. Immunohistochemistry was completed on paraffin-embedded sections as described previously (13, 14), with minor modifications. Fixed tissues were dehydrated in an ethanol series and embedded in paraffin wax. Sections were cut at 6 μm and dried onto poly-L-lysine-coated slides. For gills, sections from the trailing half of the filaments were selected for immunohistochemical staining, because they contain the highest density of ion transport cells (26). Tissue sections were deparaffinized in Citrisolv (Fisher Scientific, Pittsburgh, PA) and rehydrated in an ethanol series, followed by PBS. Endogenous peroxidase activity was inhibited by incubating with 3% H_2O_2 for 25 min at 24°C. Nonspecific binding sites on the tissues were blocked by incubating with Biogenex's (San Ramon, CA) protein block (BPB: normal goat serum with 1% bovine serum albumin, 0.09% NaN_3, and 0.1% Tween 20) for 20 min.

Preliminary experiments with antisera from all four rats suggested that two were specific (R1B2 and R2B2), with R1B2 yielding the highest signal-to-background ratios. Therefore, the remaining immunostaining was conducted with R1B2. Sections were incubated with R1B2 (diluted 1:1,000 to 1:2,000 in BPB) overnight at 4°C in a humidified chamber. Negative control sections were incubated with BPB lacking antibodies, preimmune serum, or R1B2 that was preabsorbed with 3.15 nmol/l antigen. Unbound primary antibodies were removed with a 5-min rinse in PBS. Sections were then incubated with Biogenex's (San Ramon, CA) multilink solution (biotinylated goat anti-mouse, -rabbit, -guinea pig, and -rat antibodies diluted in BPB), followed with Biogenex's horseradish peroxidase-streptavidin solution for 20 min at 24°C each. After another wash in PBS for 5 min, antibody binding was visualized by incubating with 3,3′-diaminobenzidine tetrahydrochloride (DAB) for 5 min at 24°C. Sections were then rinsed with running tap water for 5 min, dehydrated in an ethanol-Citrosolv series, and mounted with a coverslip using Permount (Fisher Scientific).

A double-labeling technique, described previously (13, 14), was used to compare the location of NHE3 immunoreactivity to Na^+/K^+-ATPase and vacuolar H^+-ATPase immunoreactivity in gills (50, 51). Gill sections were deparaffinized, hydrated, and stained with antibody R1B2 as described above. However, after treatment with DAB and rinsing with water, the sections were again blocked with BPB for 20 min and incubated with a monoclonal antibody for Na^+/K^+-ATPase (α5) or a monoclonal antibody for the E-subunit of vacuolar H^+-ATPase (E11). Concentrations were 1:10 or 1:50 for α5 and 1:10 for E11. Detection of bound antibody was done as described above, except Vector SG, which produced a blue reaction product, was used for Na^+/K^+-ATPase and Vector VIP, which produced a purple reaction product, was used for vacuolar H^+-ATPase.

Antibody α5 was developed by Dr. Douglas Fambrough and was obtained from the Developmental Studies Hybridoma Bank, which was developed under the auspices of the National Institute of Child Health and Human Development of the Department of Biological Sciences, University of Iowa (Iowa City, IA). It was made against the avian Na^+/K^+-ATPase α-subunit and binds to all isoforms. This antibody recognizes fish Na^+/K^+-ATPase and is now used widely for studies on fish branchial cells (e.g., Refs. 13, 14, 50). The monoclonal antibody for vacuolar H^+-ATPase (E11) was a gift from Stephen Gluck (Department of Medicine, University of California, San Francisco, CA). It was made against a peptide that represents the carboxy-terminal 10 residues of the bovine kidney 31-kDa E-subunit of vacuolar H^+-ATPase and has been used to localize vacuolar H^+-ATPase in fish gills (13).

Oocyte immunohistochemistry. Female *Xenopus laevis* injected with human chorionic gonadotropin were purchased from Xenopus Express (Beverly Hills, FL). Oocytes were removed and collagenase dissociated as described previously (54). The full-length stingray NHE3 cDNA was subcloned into pCR 4-TOPO (Invitrogen). Capped, sense cRNA was synthesized using a *Pme*I linearized cDNA template and the T7 mMessage mMachine kit (Ambion). Oocytes were injected with 50 nl of stingray NHE3 cRNA (0.5 μg/μl) or water and then incubated in OR_3 medium at 18°C (54). Oocytes were fixed 4–14 days after injection. The stingray NHE3 cDNA was also subcloned into pGEMHE, a *Xenopus* oocyte expression plasmid, as previously described (54, 71). For this cDNA, the expression plasmid did not seem to enhance protein expression (not shown).

Oocytes were washed with PBS, fixed using 4% paraformaldehyde in PBS at room temperature for 60 min, and processed for cryosectioning as described previously (57). Immunostaining was performed using 1:100 R1B2 antiserum and 1:500 dilution of a donkey anti-rat-Cy2 secondary antibody. Epifluorescent images were captured using a Zeiss AxioVert 25 microscope, and multichannel images were acquired with an AxioCam digital camera and AxioVision software (Carl Zeiss, Jena, Germany) (57).

Western blotting. Preliminary Western blots with antiserum R1B2 failed to label a single band, and therefore antiserum R1B2 was affinity purified with recombinant antigen using a Pierce Seize primary immunoprecipitation kit (Rockford, IL). Briefly, an affinity column was generated by coupling 100 μg of antigen (recombinant stingray NHE3 carboxyl tail; see *Antibody production*) to 100 μl of AminoLink Plus gel according to the manufacturer's protocol. Antiserum was then diluted 1:3 with Pierce Gentle Binding Buffer and incubated with the affinity column for 16 h at 4°C. After extensive washing with TBS (25 mmol/l Tris, 150 mmol/l NaCl, pH 7.2), purified antibody was eluted with Pierce Gentle Elution Buffer. The purified antibody was dialyzed in TBS overnight, and 1% bovine serum albumin and 0.02% azide were added for stability. The affinity-purified R1B2 antibody produced the same immunohistochemical labeling as unpurified R1B2 antiserum and was used for Western blot analysis.

Immunoblots were prepared from Ringer-perfused gill tissue by using a procedure modified from Choe et al. (14). Briefly, tissues were homogenized in buffer [250 mmol/l sucrose, 30 mmol/l Tris, 1 mmol/l Na_2EDTA, 5 μl/ml protease inhibitor cocktail (Sigma P8340), 100 μg/ml phenylmethylsulfonyl fluoride, pH 7.8] with a mechanical homogenizer for 30 s at maximum speed on ice. Homogenates were then centrifuged at 10,000 *g* for 10 min at 4°C to remove debris and whole nuclei. The total protein concentration was determined with the Pierce BCA assay, and Laemmli loading buffer was added (35). Protein samples (40 μg) were loaded and run in 7.5% Tris·HCl precast polyacrylamide gels (Bio-Rad, Hercules, CA) and then transferred onto polyvinylidene difluoride (PVDF) membranes. A separate

blot was prepared with 1 ng of the recombinant stingray NHE3 carboxyl tail protein and an 18% Tris·HCl precast polyacrylamide gel (Bio-Rad).

The PVDF membranes were blocked in Blotto (5% nonfat milk in TBS) for 1 h at ~24°C and then incubated in Blotto with either affinity-purified antibody R1B2 (1:20) or affinity-purified antibody R1B2 that was preincubated with 80 nmol/l antigen. Membranes were then washed with four changes (15 min each) of TBS with 0.1% Tween 20 (TBST) and incubated in goat anti-rat (Promega, Madison, WI) IgG secondary antibody (alkaline phosphatase conjugated) diluted 1:2,500 in Blotto for 1 h at ~24°C. After four more washes in TBST, the membranes were incubated in Immun-Star ECL substrate (Bio-Rad) for 5 min at 24°C. Luminescent bands were then detected with Hyperfilm-ECL (Amersham Pharmacia, Piscataway, NJ), according to the manufacturer's protocol. Finally, Western blot results were digitized with a Canon D660U flatbed scanner and Adobe Photoshop 7.0 software.

RESULTS

Molecular identification of putative transporters. In initial PCR reactions, oligonucleotide primers NHE F2 deg and NHE R1 deg supported the amplification of ~667-bp products from stingray gill cDNA that matched the size expected from vertebrate NHE nucleotide alignments. After several clones had been sequenced, it was clear that the two degenerate primers amplified three stingray NHE homologs (GenBank accession nos. AY626248, AY626249, and AY626250) that were 74.7, 69.5, and 77.1% identical to human NHE1 (BC012121), NHE2 (NM_003038), and NHE3 (NM_004174), respectively. BLAST e-values for the putative stingray NHE2 and NHE3 sequence fragments were $<10^{-75}$ for mammalian NHE2 and NHE3, respectively.

Oligonucleotide primers NK2-F1 deg and P-R1 deg supported the amplification of a ~700-bp product (AY652417) that was 75.4 and 91.4% identical to Na^+/K^+-ATPase subunit α1 from human (NM_000701) and torpedo ray (*Torpedo californica*; X02810), respectively. BLAST e-values for the putative stingray Na^+/K^+-ATPase subunit α1 sequence fragment were also $<10^{-75}$ for the mammalian ortholog.

Distribution of putative transporters. Multiplex RT-PCR with cDNA from gill, stomach, kidney, spiral value intestine, and rectal gland was conducted to determine the distribution of putative stingray NHE2, NHE3, and Na^+/K^+-ATPase α1 mRNA in epithelial transport tissues. After 30 cycles of PCR with the putative stingray NHE2- and NHE3-specific primers (NHE2 F1-NHE2 R1 and NHE3 F1-NHE3 R1), the expected 470- and 431-bp products were the most abundant for spiral valve intestine, followed by gill and kidney (Fig. 1). Faint bands were also visible for rectal gland and stomach when gel lanes were overloaded (unpublished observation). After 32 cycles of PCR with the putative stingray Na^+/K^+-ATPase α1-specific primers (NKA F1-NKA R1), the expected 428-bp product was most abundant for rectal gland, followed by (in decreasing order) spiral valve, kidney, gill, and stomach (Fig. 1). In all cases, the 315-bp product expected from the 18S internal control primers was observed for all tissues, at roughly equivalent levels (Fig. 1).

Quantitative real-time PCR. The mRNA expression of NHE3 and Na^+/K^+-ATPase α1 in the gills from freshwater-acclimated stingrays was 116 and 61% greater than in gills from seawater stingrays, respectively (Fig. 2*A*). Alternatively, there was no difference in expression of NHE2 between the two salinities. There was also no difference in expression of mRNA for any of the transporters in the gills from normocapnic and hypercapnic stingrays after either 2 or 4 h of exposure (Fig. 2*B*). The relative expression level of NHE3 and Na^+/K^+-ATPase α1 mRNA were well correlated in the gills of seawater control stingrays ($r^2 = 0.758$, slope = 0.46, and $P < 0.0001$) (Fig. 2*C*). Alternatively, the relative expression level of NHE2 mRNA was not correlated to either NHE3 or Na^+/K^+-ATPase α1 (unpublished observations).

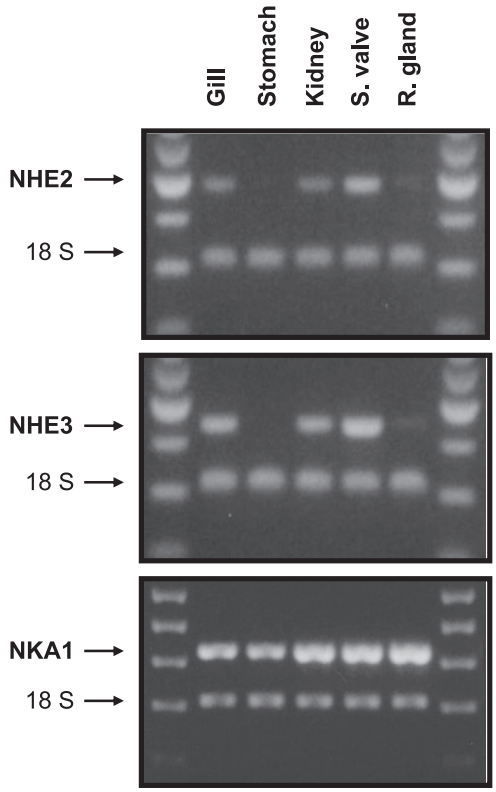

Fig. 1. Multiple-tissue relative quantitative PCR. Multiplex PCRs with primer pairs for putative Na^+/H^+ exchanger 2 (NHE2), NHE3, or Na^+/K^+-ATPase α1 (NKA1) fragments and a 315-bp fragment of the 18S ribosomal RNA were conducted with randomly primed stingray cDNA as a template. The 470- and 431-bp NHE2 and NHE3 fragments were amplified, in decreasing order, from spiral valve, gill, kidney, and rectal gland. Faint bands for NHE2 and NHE3 were also visible for stomach, when lanes were overloaded (unpublished observation). The 428-bp NKA1 fragment was amplified, in decreasing order, from rectal gland, spiral valve, kidney, gill, and stomach. 18S was amplified approximately equally from cDNA of all tissues. One hundred-base pair ladder molecular weight markers were run in the lanes to the *left* and *right* of samples. NKA1, Na^+/K^+-ATPase α1; s. valve, spiral valve; r. gland, rectal gland.

Molecular identification of NHE3. Because NHE3 expression was greater in freshwater-acclimated stingrays than in seawater stingrays, we completed the cloning and sequencing of NHE3 so that it could be further characterized. The complete putative stingray NHE3 cDNA (accession no. AY626250) contains 2,744 nucleotides with a 2,511-nucleotide open reading frame that codes for an 837-amino acid protein (Fig. 3). The likely start codon (ATG) is 75 nucleotides downstream from the 5′ end of the cDNA obtained by RACE, and a likely in-frame stop codon (TAA) is 159 nucleotides upstream from the 3′ end of the cDNA. A transcript cleavage sequence (AATAAA) is 43 nucleotides upstream from a polyA tail. PCR with primers just upstream from the start codon and

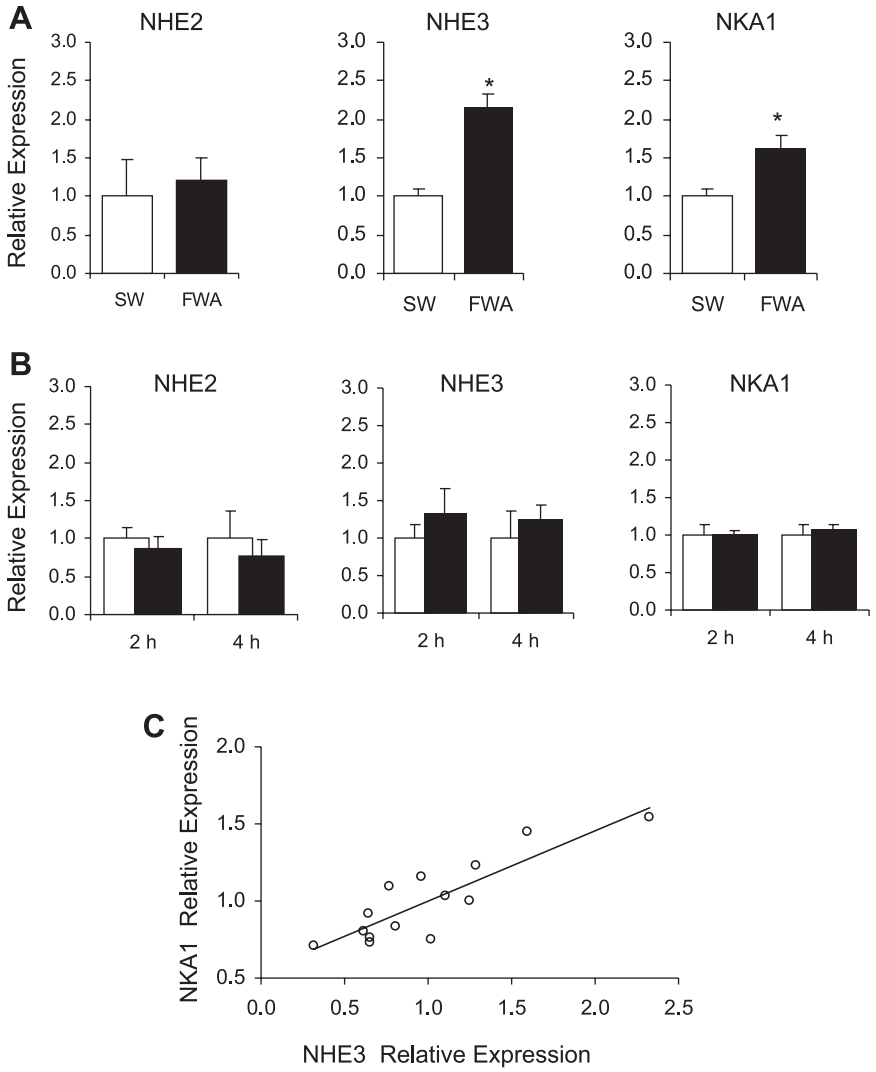

Fig. 2. Quantitative real-time PCR. Relative expression of putative transporters was measured in gills during freshwater acclimation (*A*) and hypercapnia (*B*). Open bars represent means for control animals (seawater in *A* and normocapnia in *B*), and closed bars represent means for treated animals (freshwater acclimated in *A* and hypercapnia in *B*). Data are plotted as means + SE; $n = 4$ for *A* and 5 for *B*. *$P < 0.05$. *C*: relative expression of Na^+/K^+-ATPase α1 and NHE3 mRNA in gills from control stingrays was highly correlated ($r^2 = 0.758$, slope = 0.46, $P < 0.0001$). SW, seawater; FWA, freshwater acclimated.

just downstream from the stop codon amplified a product of the expected 2,606 base pairs, and sequencing of this product verified alignment of the complete cDNA. The complete stingray protein grouped with other vertebrate NHE3 homologs in phylogenetic analysis (Fig. 4). In separate trees that included human NHE6–8, NHE1–5 formed one group and NHE6–8 formed another distantly related group (unpublished observation).

In situ hybridization and immunological analysis. Antisense RNA *probes 1* and *19* labeled specific epithelial cells in the filament of seawater stingrays (Fig. 5), and no labeling was observed when sections were incubated with the corresponding sense probes (Fig. 5*A*). Staining of serial sections demonstrated that riboprobes for NHE3 labeled cells that are immunoreactive for Na^+/K^+-ATPase (Fig. 5, *D* and *E*).

The anti-stingray NHE3 antiserum, RIB2, reacted strongly with a subpopulation of epithelial cells in stingray gills (Fig. 6*A*). In seawater control stingrays, staining was limited to the apical side of cuboidal epithelial cells in the filament and at the base of lamellae (Fig. 6*A*). No staining was observed when sections were incubated with BPB, preimmune serum, or R1B2 antibody preincubated with antigen (Fig. 6*B*). We stained for NHE3 and Na^+/K^+-ATPase or NHE3 and vacuolar H^+-ATPase in the same gill sections to determine whether NHE3 immunoreactivity colocalized with either of the ATPase ion pumps. NHE3 immunoreactivity was always in the same cells as Na^+/K^+-ATPase immunoreactivity (Fig. 6*C*). Within these double-labeled cells, Na^+/K^+-ATPase immunoreactivity was confined to the basolateral region and NHE3 staining was always in the apical region (Fig. 6*C*). Alternatively, NHE3 immunoreactivity was never in the same cells as vacuolar H^+-ATPase immunoreactivity (Fig. 6*D*).

Antiserum R1B2 labeled *Xenopus* oocytes that were injected with stingray NHE3 cRNA but not oocytes injected with water (Fig. 7, *A–D*). Most of the staining was intracellular (Fig. 7*D*), suggesting that additional proteins and/or signals are required to locate the majority of stingray NHE3 to the plasma membrane (Fig. 6). The affinity-purified R1B2 antibody labeled the 25-kDa recombinant stingray NHE3 carboxyl tail protein in Western blots (Fig. 7*E*). The affinity-purified antibody also produced the same immunohistochemical labeling as antiserum (not shown) and labeled a single 87-kDa protein on Western blots of stingray gill proteins (Fig. 7*F*). Preincubation of the antibody with excess antigen blocked this labeling (Fig. 7*F*).

There were marked qualitative differences in the location and abundance of NHE3-immunoreactive cells between the

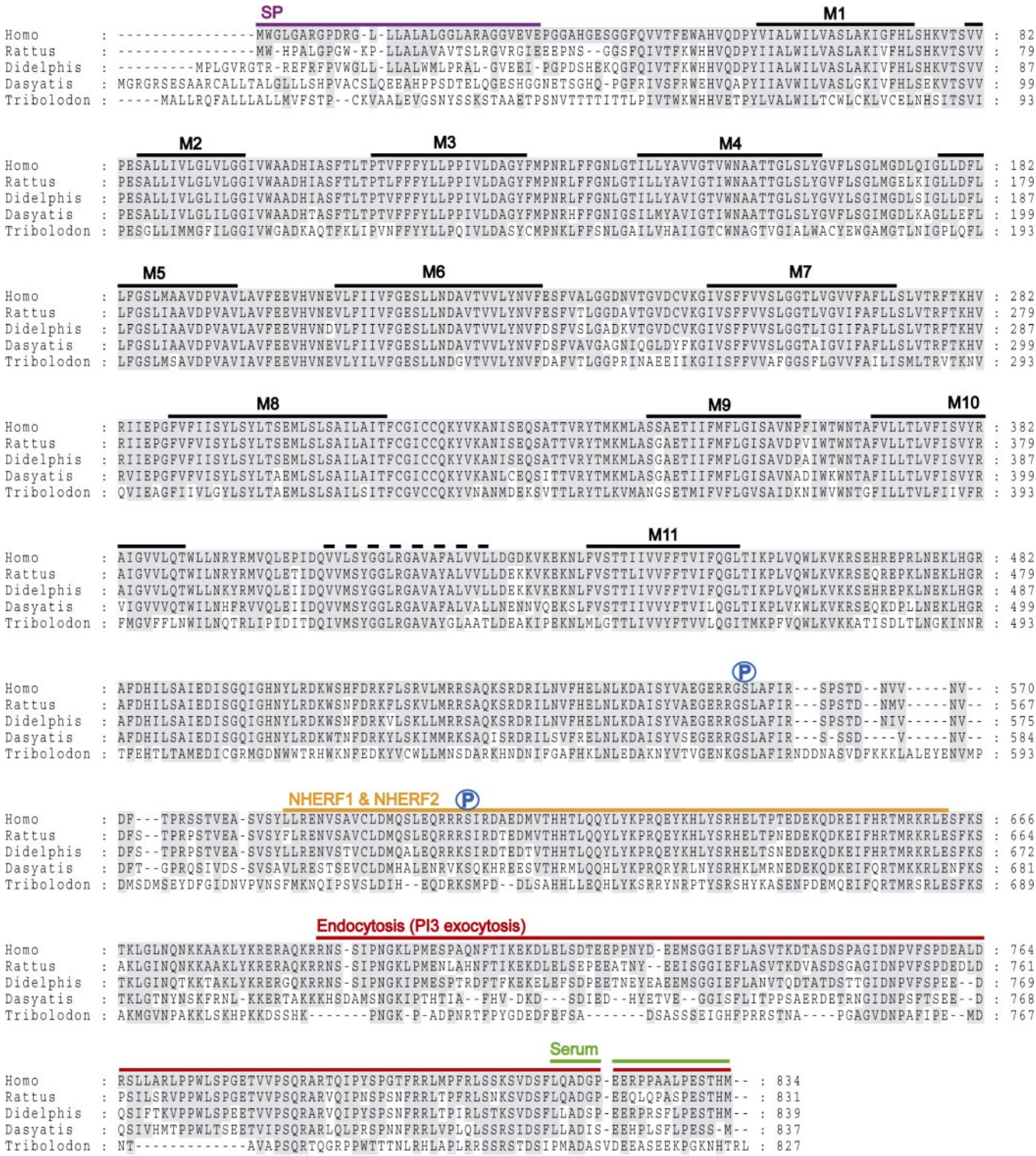

Fig. 3. Amino acid alignment of the putative stingray NHE3 with NHE3 from other vertebrates (labeled by genus). Gaps (dashes) were introduced to maintain alignment. All amino acids that are identical or similar to those of the human NHE3 are shaded (Blosum 62 scoring matrix with the following amino acid groups considered similar: DN, EQ, ST, KR, FYW, and LIVM). Putative transmembrane domains are labeled M1 to M11, and an additional hydrophobic region is marked with a bold dashed line. Serine phosphorylation sites of mammalian NHE3 that partially mediate the inhibitory effects of cAMP are marked with a blue P and are conserved in all homologs (41). A region known to interact with NHE regulatory factors 1 and 2 (NHERF1 and 2) and partially mediate the inhibitory effects of cAMP (72) is marked with an orange line and is well conserved in all homologs. A terminal carboxyl region of mammalian NHE3 known to mediate endocytosis of NHE3-containing vesicles is marked with a red line (1). Phosphatidylinositol 3-kinase (PI3) activation promotes exocytosis of NHE3 via the same region (1). This region is well conserved in the mammals, mostly conserved in stingray, but less conserved in dace (*Tribolodon,* teleost). Finally, a region known to mediate serum stimulation of NHE3 activity is marked with a green line and is well conserved in all the vertebrates except dace (37). GenBank accession nos. are as follows: *Homo*, NP_004165; *Rattus*, NP_036786; *Didelphis*, Q28362; *Dasyatis*, AAT45738; and *Tribolodon*, BAB83083.

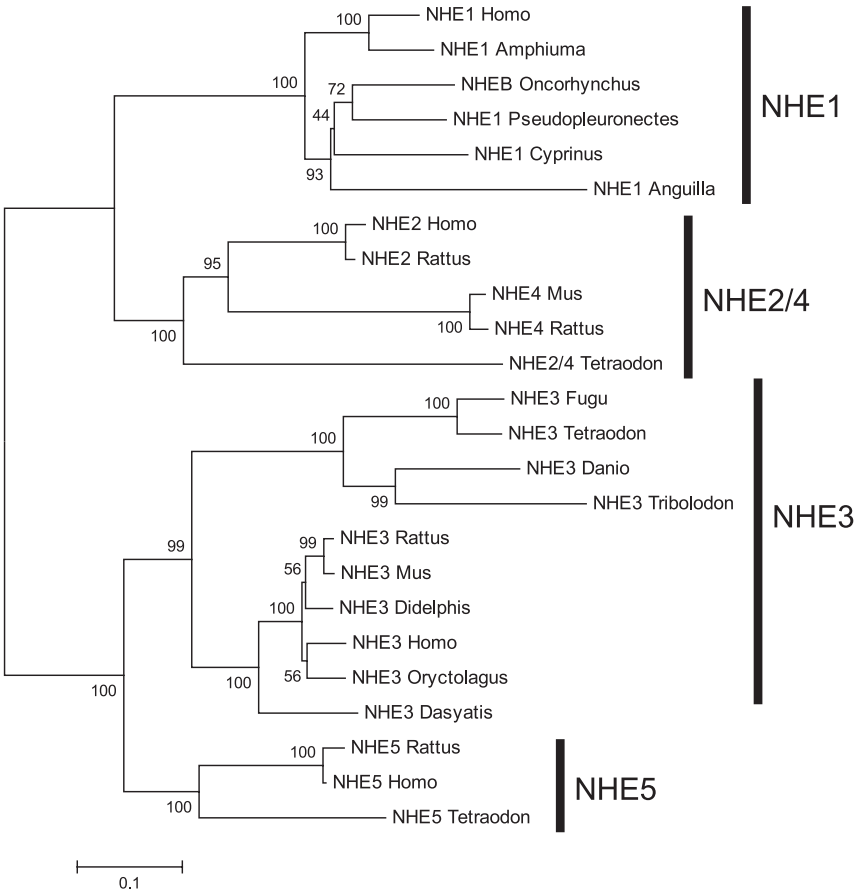

Fig. 4. Phylogenetic tree of cell surface NHE homologs (NHE1–5) demonstrating that NHE3 forms 2 subgroups, 1 that includes the teleosts and another that includes mammals and elasmobranchs. Database searches were used to find NHE3 orthologs in the teleosts, *Fugu*, *Tetraodon*, and *Danio*. The tree was constructed using the neighbor-joining method with Poisson correction, and numbers indicate bootstrap values for 1,000 replicates. All homologs are labeled by genus. GenBank accession nos. are as follows, from *top* to *bottom*: NHE1: *Homo*, NP_003038; *Amphiuma*, AAD33928; *Onchorhynchus*, Q01345; *Pseudopleuronectes*, AAO44956; *Cyprinus*, CAB45232; and *Anguilla*, CAB45085; NHE2/4: *Homo*, NP_003039; *Rattus*, P48763; *Mus*, NP_796058; *Rattus*, NP_775121; and *Tetraodon*, scaffold 14781; NHE3: *Fugu*, Genscan_5486; *Tetraodon*, scaffold 7101; *Danio*, AL954769; *Tribolodon* (Osorezan dace), BAB83083; *Rattus*, NP_036786; *Mus*, XP_127434; *Didelphis* (opossum), Q28362; *Homo*, NP_004165; *Oryctolagus*, P26432; and *Dasyatis*, AAT45738; NHE5: *Rattus*, NP_620213; *Homo*, NP_004585; and *Tetraodon* (green pufferfish), scaffold 14611. Bar represents 10% replacement of amino acids per cite.

salinity treatment groups (Figs. 8 and 9). In seawater stingrays, one to two NHE3-immunoreactive cells were usually in the filamental epithelium between adjacent lamellae (Fig. 8*A*). In freshwater-acclimated stingrays, two to three NHE3-immunoreactive cells were in the filamental epithelium between adjacent lamellae, but some were also observed on the base of the lamellae (Fig. 8*B*). In freshwater stingrays, many NHE3-immunoreactive cells were in the lamellar epithelium and not in the filamental epithelium (Fig. 8*C*). In all salinity treatments, NHE3 immunoreactivity was in the apical region of cells that also contained Na^+/K^+-ATPase immunoreactivity in the basolateral region (Fig. 9).

DISCUSSION

Our study is the first to use molecular and immunological techniques to demonstrate that an NHE3 homologous to that of mammalian renal proximal tubules and intestines is present in the apical side of Na^+/K^+-ATPase-rich epithelial cells in elasmobranch gills, where it may function in systemic Na^+ absorption and H^+ secretion. These conclusions are based on our molecular identification of an NHE3 ortholog in stingray gills, demonstration of greater mRNA expression of NHE3 in freshwater than in seawater, and localization of NHE3 mRNA and protein in Na^+/K^+-ATPase-rich cells.

Molecular identification of stingray NHE2/4 and NHE3. The phylogenetic analysis of our full-length sequence with available NHE sequences demonstrates that it is likely an elasmobranch ortholog of mammalian NHE3 (human SCL9A3). The apparent size of 87 kDa on Western blots (Fig. 7*B*) is the same size as NHE3 in rat (30) and matches the predicted size of stingray NHE3 minus a predicted NH_2-terminal signal peptide (SignalP 3.0) (20). Our stingray sequence is the earliest NHE3 ortholog sequenced to date, and the high homology of the stingray and mammalian NHE3s (>70% identical amino acids) suggests that NHE3 has changed very little in the elasmobranch and tetrapod lineages (including mammals) since the cartilaginous fishes separated from the rest of the vertebrate linage more than 400 million years ago (17). The activity of NHE3 in mammals is regulated by phosphorylation, protein trafficking, and regulatory proteins via the carboxyl, hydrophilic region (41). Interestingly, most of the regulatory, carboxyl regions of stingray and mammalian NHE3s are well conserved (Fig. 3), suggesting that the elasmobranch NHE3 can be regulated by similar pathways and that these control mechanisms were needed early in vertebrate evolution. Unexpectedly, the stingray NHE3 grouped closer to the mammalian NHE3s than the teleost NHE3s in phylogenetic analysis (Fig. 4). Teleosts, which include *Fugu*, *Tetraodon*, *Danio,* and *Tribolodon*, are in the sister group to the tetrapod lineage (including mammals) and share a more recent common ancestor with mammals than elasmobranchs (43). Therefore, the divergence of the teleost NHE3 sequences is contrary to the well-established phylogeny of major vertebrate groups and suggests that NHE3 evolved rapidly in the teleosts since they separated from the tetrapod lineage more than 380 million years ago (43). Most of the divergence has occurred in the regulatory carboxyl tail of teleost NHE3 (Fig. 3), suggesting that teleosts may regulate NHE3 activity by different cellular

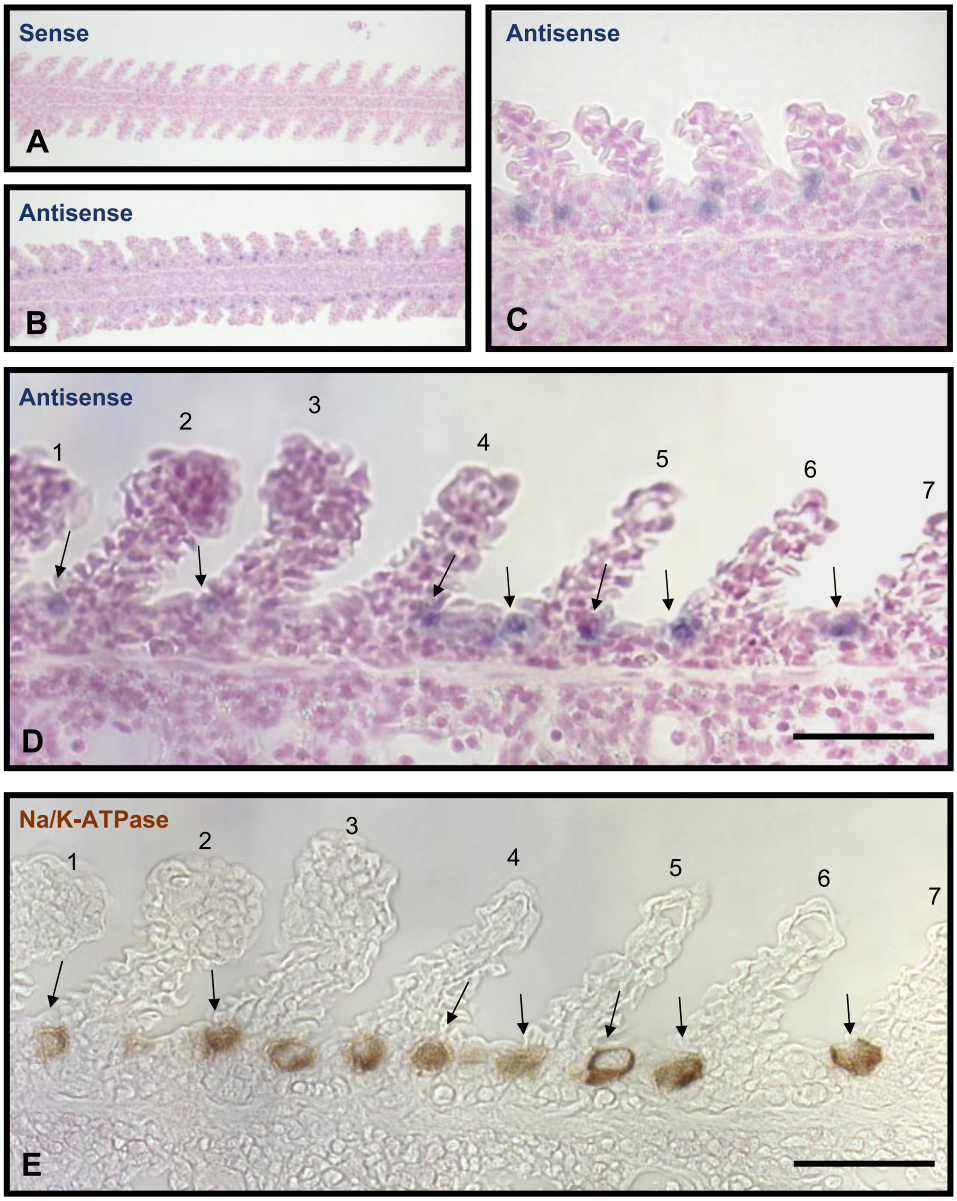

Fig. 5. Representative light micrographs of gill sections from Atlantic stingrays that demonstrate the localization of NHE3 mRNA. Gill sections were incubated with sense (*A*) and antisense (*B* and *C*) digoxigenin-labeled RNA *probe 19*, and signal was visualized with nitro blue tetrazolium/5-bromo-4-chloro-3-indolylphosphate. Antisense probes labeled specific epithelial cells in the gill filament (area at *bottom* of the sections; *D*) that were also immunoreactive for Na^+/K^+-ATPase (*E*). Sense probes did not produce a signal (*A*). In situ hybridization sections were counterstained with Kernechtrot (nuclear fast red). Scale bars, 50 μm.

signaling events than those used in mammals and elasmobranchs. For example, although three serine phosphorylation sites are conserved between teleosts and mammals, much of the region needed for control of endocytosis and exocytosis (1) has diverged in teleosts (Fig. 3).

Interestingly, our data suggest that NHE2 and NHE4 of mammals diverged recently, after the division of the teleost and tetrapod lineages (Fig. 4). In phylogenetic analyses of sequence fragments that included our putative stingray NHE2 sequence fragment, mammalian NHE2 and NHE4 always grouped together, separately from the stingray and teleost homologs (unpublished observations). Consequently, even though the fish homologs are slightly more homologous with NHE2 (~50% identical amino acids) than with NHE4 (~40% identical amino acids), they should be named NHE2/4, because they may have characteristics that are a blend of both isoforms. In mammals, NHE4 is expressed in the basolateral membranes of renal cells that lack detectable levels of NHE1 activity, where it may regulate intracellular pH and volume, and NHE2 is expressed in the apical membranes of renal and gastrointestinal cells, where it may participate in secretory functions (46). Further work is needed to characterize NHE2/4 in fishes to provide a reference point to understand the recent divergence of function and sequence between mammalian NHE2 and NHE4.

The distribution of NHE2/4 and NHE3 mRNA in stingrays is consistent with absorptive functions in epithelial tissues. Although little functional data are available for the spiral valve intestine, the high expression of NHEs in this tissue suggests that it may be responsible for ion and fluid absorption similar to that in mammalian small intestines. Although we previously demonstrated that the kidneys of Atlantic stingrays made no contribution to whole animal net acid secretion (11), the high expression in this tissue suggests a $NaHCO_3$-reabsorptive function similar to that in mammalian kidneys.

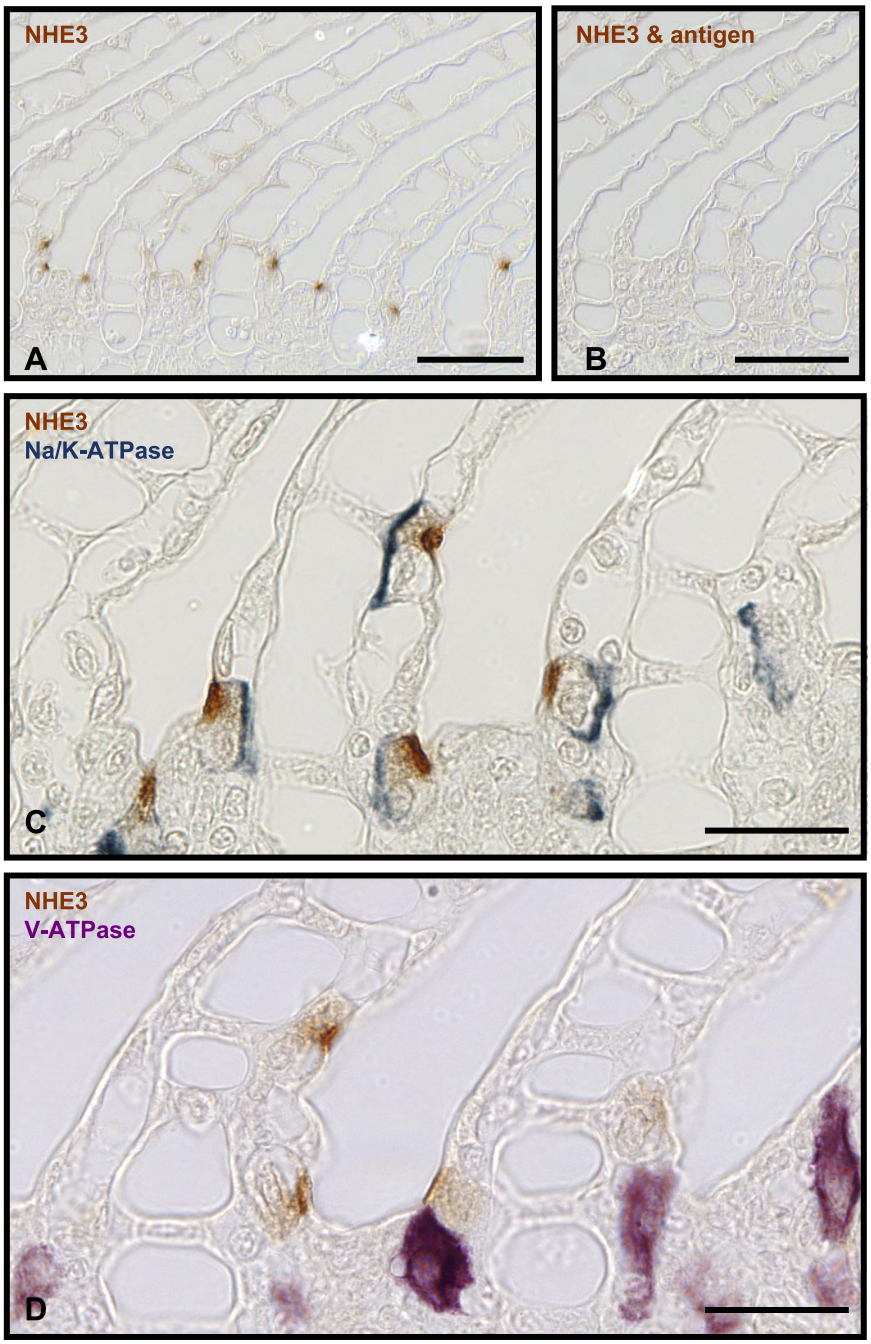

Fig. 6. Representative light micrographs of gill sections from Atlantic stingrays that demonstrate the localization of NHE3 protein in seawater. Gill sections were incubated with antiserum R1B2 (*A*), antiserum R1B2 and antigen (*B*), antiserum R1B2 and antibody α5 (*C*), or antiserum R1B2 and antibody E11 (*D*). Peroxidase substrates used to label antibodies were brown (NHE3), blue (Na^+/K^+-ATPase α1), and purple [vacuolar H^+-ATPase E subunit (V-ATPase)]. No immunolabeling was observed in negative control sections that were incubated with R1B2 and excess antigen followed by multilink (anti-mouse, -rabbit, and -donkey) secondary antibodies (*B*). However, strong immunolabeling occurred in the apical regions of a population of epithelial cells with antiserum R1B2 (*A*). In double-labeling experiments, immunolabeling with antiserum R1B2 was always in cells with basolateral Na^+/K^+-ATPase but never in cells with vacuolar H^+-ATPase (*C* and *D*). Scale bars, 50 (*A* and *B*) or 20 μm (*C* and *D*).

Mechanisms of acid secretion and Na^+ absorption. Pharmacological, immunological, and molecular studies have suggested two potential mechanisms of Na^+ absorption and H^+ secretion in fish gills: *1*) an apical vacuolar H^+-ATPase electrically linked to Na^+ absorption via an apical Na^+ channel and *2*) electroneutral exchange of Na^+ and H^+ via proteins of the NHE family (16, 21, 40). On the basis of thermodynamic considerations of ion gradients, it has been suggested that an apical NHE is not possible in freshwater, where the Na^+ concentration is usually <1 mmol/l (39). Alternatively, the vacuolar H^+-ATPase/Na^+ channel mechanism was favored because it is a primary active mechanism and because subunits of the proton pump were localized to the apical side of branchial epithelial cells of some teleosts in freshwater (*Onchorynchus mykiss, O. kisutch,* and *Oreochromis mossambicas)* (38, 49, 59, 68, 69). However, more recent studies on elasmobranchs (25, 51, 60) and even a teleost (*Fundulus heteroclitis*) (33) have demonstrated that vacuolar H^+-ATPase is in the basolateral membranes of gill epithelia in at least some fishes, where they may have a role in base secretion and Cl^- absorption instead of acid secretion and Na^+ absorption.

Our demonstration of greater NHE3 mRNA expression and immunoreactivity in freshwater-acclimated stingray gills relative to seawater stingray gills suggests that an NHE can absorb Na^+ from a hypoionic environment. Our clear apical localization of NHE3 in Na^+/K^+-ATPase-rich cells is the first dem-

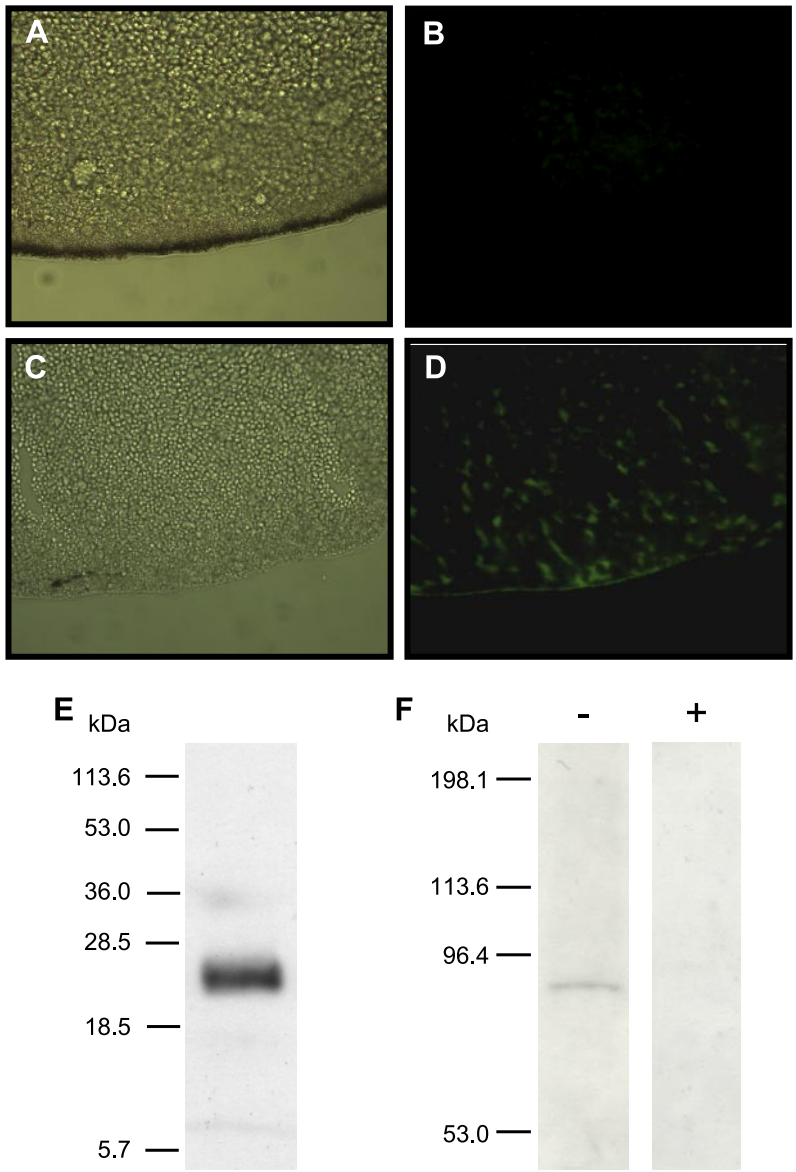

Fig. 7. Antibody specificity controls. *Xenopus* oocytes were injected with water (*A* and *B*) or stingray NHE3 cRNA (*C* and *D*) and were incubated with antiserum R1B2 (green). Representative light (*A* and *C*) and fluorescence (*B* and *D*) micrographs are included. Western blots include recombinant stingray NHE3 carboxy tail protein (*E*) or stingray gill protein (*F*) incubated with affinity-purified antibody R1B2. Stingray gill protein blots were incubated with (+) or without (−) preincubation with excess antigen.

onstration of NHE immunoreactivity in a freshwater elasmobranch and strongly supports this predicted function (Figs. 6, 8, and 9). Presumably, high levels of Na^+/K^+-ATPase activity would be required in the same cell to lower intracellular Na^+ concentration enough to allow Na^+ entry from the environment. Our demonstration of increased Na^+/K^+-ATPase mRNA and immunoreactivity confirms earlier findings of greater Na^+/K^+-ATPase activity and protein levels in freshwater than in seawater (50). A recent study demonstrated apical NHE3 immunoreactivity in the gills of freshwater Osorezan dace (*Tribolodon hakonensis*), a unique teleost that lives in a highly acidic environment (29). That study demonstrated a large increase in NHE3 mRNA and protein expression when dace were transferred from neutral to acidic water, suggesting a function in systemic acid secretion. However, NHE3 expression was not compared with higher salinities, and therefore the effect of salinity on dace NHE3 is unknown.

Before the availability of full-length fish cDNA sequences, a single, heterologous antibody for NHE3 (1380) was used to detect immunohistochemical reactivity in three teleosts (*O. mykiss, Pseudolabrus tetrious*, and *Periophthalmodon schlosseri*) and two elasmobranchs (*Mustelus antarcticus* and *Squantina australis*) (21, 22, 67). Unfortunately, the cellular (pavement or mitochondrion-rich cell) and subcellular (apical, cytoplasmic, or basolateral) localization was variable between species, and therefore further work with homologous antibodies is needed before definitive conclusions can be made about NHE3 localization in those species. In retrospect, there is a low degree of sequence identity between the carboxyl region of rabbit NHE3 used to generate antibody 1380 and the corresponding regions of the fish proteins (29/85 amino acids for NHE3 of dace and 45/85 amino acids for NHE3 of stingray) that may explain some of the variability in staining. An antibody generated against an internal region of rat NHE3 (666) was used to detect immunoreactivity on Western blots of gill proteins from an elasmobranch (*Raja erinacea*), but localization was not achieved (12).

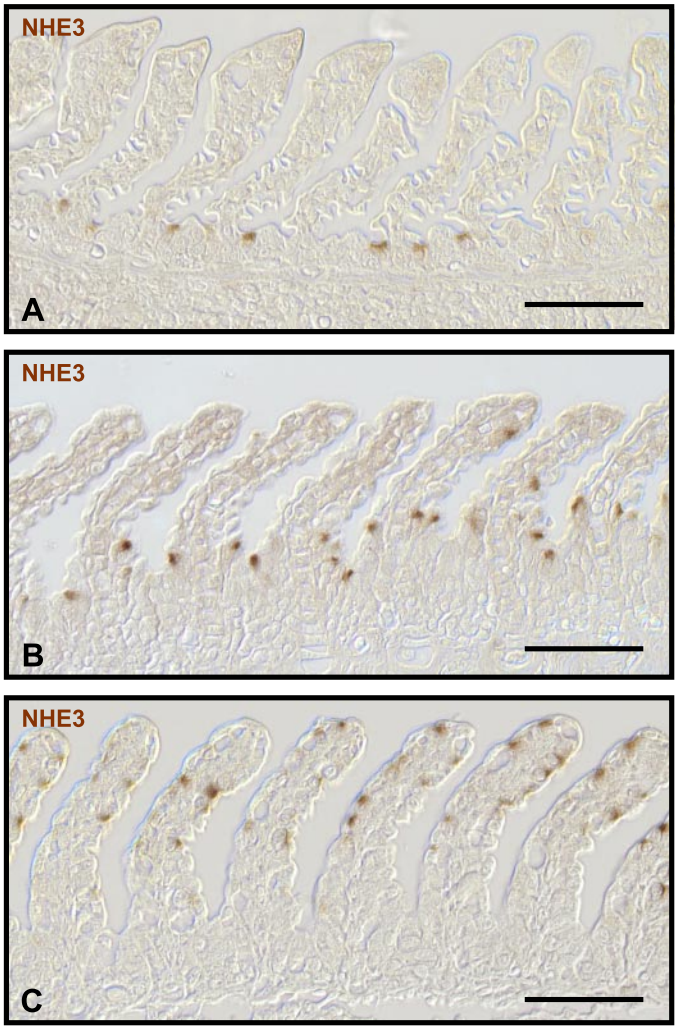

Fig. 8. Representative light micrographs of Atlantic stingray gill sections from seawater (*A*), freshwater-acclimated (*B*), and freshwater stingrays (*C*) incubated with antiserum R1B2 (brown). The location of immunoreactive cells was different in the 3 groups, ranging from mostly in the filament in seawater stingrays to mostly in the lamellae in freshwater stingrays. Immunoreactivity was in the apical region of cells in all salinity treatments (*A–C*). Scale bars, 50 μm.

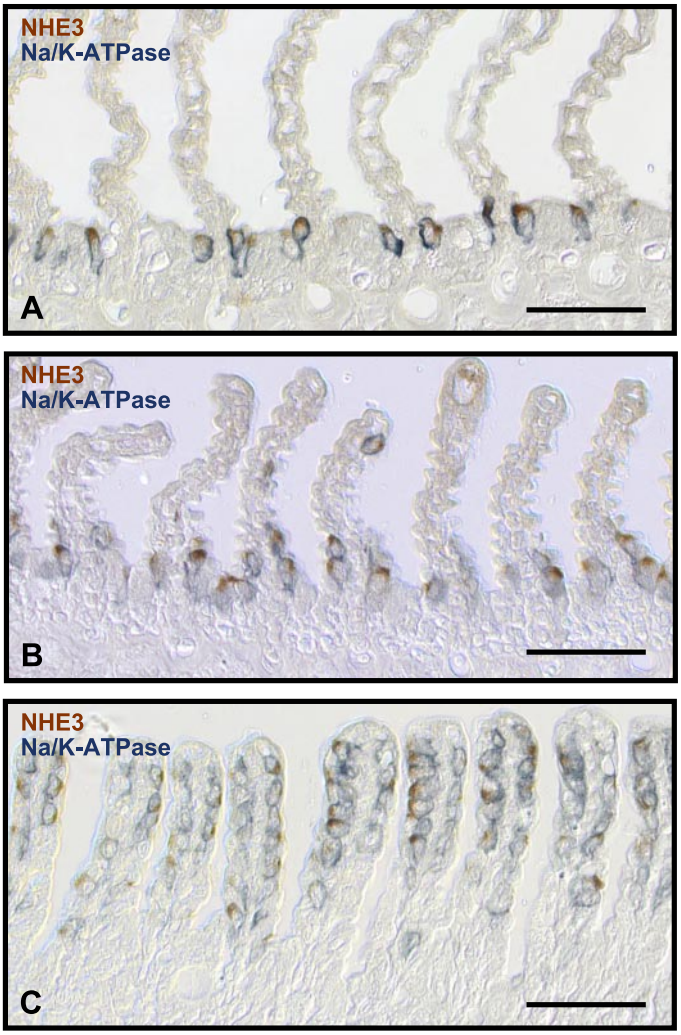

Fig. 9. Representative light micrographs of Atlantic stingray gill sections from seawater (*A*), freshwater-acclimated (*B*), and freshwater stingrays (*C*) incubated with antiserum R1B2 (brown) and antibody α5 (blue). R1B2 immunoreactivity was always in the apical region of cells with basolateral Na^+/K^+-ATPase, regardless of salinity treatment (*A–C*). Scale bars, 50 μm.

In previously published experiments, we demonstrated that in vivo net acid excretion rates from seawater stingrays increased to their highest values (5 times control excretion rates) during the first 4 h of hypercapnia and that blood pH decreased to its lowest value after 2 h of hypercapnia (11). In the current study, there were no repeatable changes in expression of NHE2/4, NHE3, or Na^+/K^+-ATPase during these time intervals. This lack of an increase in mRNA expression for these transporters during hypercapnia suggests that either *1*) acid secretion is accomplished via other transporters that we have not considered or *2*) one or more of these transporters are involved but that stimulation of acid secretion is via posttranslational regulation during an acute acidosis such as hypercapnia (11). H^+/K^+-ATPases and vacuolar H^+-ATPase (27, 44) are the only other H^+ transporters known to mediate epithelial acid secretion in vertebrates. However, in a previously published study of the same animals, we demonstrated that H^+/K^+-ATPase α1 mRNA expression was also unaffected by

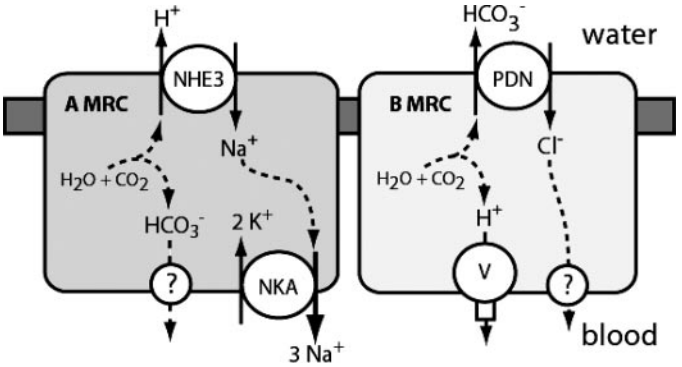

Fig. 10. Model of hypothesized ion and acid-base transport mechanisms in the gills of Atlantic stingrays based on previous immunocytochemical results (50, 51, 53) and the quantitative PCR and localization results of the current study. There are 2 populations of cells that appear to be specialized for transepithelial ion and acid-base transport: A-type mitochondrion-rich cells (A MRC) and B-type mitochondrion-rich cells (B MRC). Electrogenic transport is indicated with unequal arrow weights. Solid arrows indicate facilitated transport, and broken arrows indicate diffusion. V, vacuolar H^+-ATPase; PDN, pendrin-like anion exchanger.

hypercapnia (14). Finally, vacuolar H^+-ATPase is localized to the basolateral membranes of elasmobranchs (25, 51, 60) and therefore cannot secrete acid directly into environmental water. Although our data did not identify a transporter that was upregulated during acidosis, they did suggest that NHE3 might be the most abundant putative acid transporter that we measured. For example, by using quantified plasmid DNA for our standard curves, we were able to calculate that the relative cDNA transcript copies per unit volume of total gill cDNA were 334.8 ± 28.4, 73.2 ± 36.1, and 1.0 ± 0.2 for NHE3, NHE2/4, and H^+/K^+-ATPase α1, respectively. Although these values may not strictly reflect mRNA abundance in native gill tissue because of variable reverse transcription rates (58), they and the apical localization of NHE3 protein do lead us to hypothesize that NHE3 may be the largest quantitative contributor to acid secretion.

We were unable to determine the potential function of NHE2/4 in the gills, because its expression did not change with either salinity or hypercapnic manipulations. Similarly, NHE3 is clearly responsible for the majority of $NaHCO_3$ reabsorption in mammalian renal tubules, but the exact functions of NHE2 in mammalian renal tubules are still being determined (46). Although NHE2 knockout mice have no measurable renal absorptive malfunctions (36, 70), a recent study showed that NHE2 is important for bicarbonate reabsorption in mammalian distal nephron segments under conditions of high distal bicarbonate delivery (4).

Stingray gill model. Our group previously identified a subpopulation of mitochondrion-rich cells in the gills of elasmobranchs that express high levels of Na^+/K^+-ATPase in the basolateral membranes (50). The current study is the first to use homologous antibodies to demonstrate apical immunoreactivity for NHE3 in these cells. Together with the high homology of our stingray NHE3 to mammalian NHE3 and the increased expression in freshwater, the colocalization of apical NHE3 and basolateral Na^+/K^+-ATPase strongly suggest that this cell functions for Na^+ absorption and H^+ secretion similarly to renal proximal tubule cells of mammals (3). In this scenario, Na^+/K^+-ATPase in the basolateral membrane creates a low intracellular Na^+ concentration that provides a gradient for Na^+ to enter through the apical membrane via NHE3 (Fig. 10). In addition, a yet to be identified basolateral mechanism for HCO_3^- efflux toward the blood can lower the intracellular pH and help make apical Na^+/H^+ exchange favorable.

The mechanism for Cl^- absorption/HCO_3^- secretion was suggested by previous studies that used heterologous antibodies to localize pendrin immunoreactivity to the apical side of vacuolar H^+-ATPase-rich cells (25, 53). In this cell, we predict that vacuolar H^+-ATPase alkalizes the intracellular space by removing H^+ across the basolateral membrane (Fig. 10). The alkaline environment then generates intracellular HCO_3^- that is secreted across the apical membrane in exchange for Cl^- via a putative pendrin-like anion exchanger. This scenario is similar to B-type intercalated cells of mammal renal collecting ducts (55).

In summary, we have sequenced the first putative NHE3 ortholog from an elasmobranch, which dates the origin of NHE3 to at least before the division of bony and cartilaginous fishes. The stingray NHE3 shares a high degree of homology with mammalian NHE3 and is expressed in tissues that are expected to absorb Na^+. We have shown that expression of NHE3 mRNA increased in the gills during acclimation to low environmental salinity and that NHE3 protein is expressed exclusively in the apical side of mitochondrion-rich cells that have high levels of basolateral Na^+/K^+-ATPase. Taken together, these data are strong evidence that the mechanism for Na^+ absorption and acid secretion in the gills of elasmobranchs is similar to the mechanism of $NaHCO_3$ reabsorption in the renal proximal tubules of mammals.

ACKNOWLEDGMENTS

We thank Michael Myamoto and Andrew Diamanduros for assistance with phylogenetic analysis of the NHE homologs. We also thank Kristina Choe and Henry Coulter for assisting in the collection of stingrays.

GRANTS

This material is based on work supported by National Science Foundation Grants IBN-0089943 (to D. H. Evans), IBN-0413427 (to K. P. Choe), and IBN-0111073 (to J. B. Claiborne), by Ministry of Education, Culture, Sports, Science, and Technology, Japan Grants 14104002 (to S. Hirose) and 16710145 (to A. Kato), and by National Institute of Diabetes and Digestive and Kidney Diseases Grant DK-56218 (to M. F. Romero). An East Asia and Pacific Summer Institute Program fellowship from the Japan Society for the Promotion of Science was also critical to completing this study.

REFERENCES

1. **Akhter S, Cavet ME, Tse CM, and Donowitz M.** C-terminal domains of Na^+/H^+ exchanger isoform 3 are involved in the basal and serum-stimulated membrane trafficking of the exchanger. *Biochemistry* 39: 1990–2000, 2000.
2. **Amemiya M, Loffing J, Lotscher M, Kaissling B, Alpern RJ, and Moe OW.** Expression of NHE3 in the apical membrane of rat renal proximal tubule and thick ascending limb. *Kidney Int* 48: 1206–1215, 1995.
3. **Aronson PS.** Ion exchangers mediating NaCl transport in the renal proximal tubule. *Cell Biochem Biophys* 36: 147–153, 2002.
4. **Bailey MA, Giebisch G, Abbiati T, Aronson PS, Gawenis LR, Shull GE, and Wang T.** NHE2-mediated bicarbonate reabsorption in the distal tubule of NHE3 null mice. *J Physiol* 561: 765–775, 2004.
5. **Biemesderfer D, Pizzonia J, Abu-Alfa A, Exner M, Reilly RF, Igarashi P, and Aronson P.** NHE3: a Na^+/H^+ exchanger isoform of renal brush border. *Am J Physiol Renal Fluid Electrolyte Physiol* 265: F736–F742, 1993.
6. **Biemesderfer D, Rutherford PA, Nagy T, Pizzonia JH, Abu-alfa AK, and Aronson PS.** Monoclonal antibodies for high-resolution localization of NHE3 in adult and neonatal rat kidney. *Am J Physiol Renal Physiol* 273: F833–F840, 1997.
7. **Bigelow HB and Schroeder WC.** *Fishes of the Western North Atlantic. Memoir of the Sears Foundation for Marine Research*. New Haven, CT: Yale University Press, 1953.
8. **Brett CL, Donowitz M, and Rao R.** Evolutionary origins of eukaryotic sodium/proton exchangers. *Am J Physiol Cell Physiol* 288: C223–C239, 2005.
9. **Bustin SA.** Quantification of mRNA using real-time reverse transcription PCR (RT-PCR): trends and problems. *J Mol Endocrinol* 29: 23–39, 2002.
10. **Chambrey R, Warnock DG, Podevin RA, Bruneval P, Mandet C, Belair MF, Bariety J, and Paillard M.** Immulocalization of Na^+/H^+ exchanger isoform NHE2 in rat kidney. *Am J Physiol Renal Physiol* 275: F379–F386, 1998.
11. **Choe K and Evans D.** Compensation for hypercapnia by a euryhaline elasmobranch: effect of salinity and roles of gills and kidneys in fresh water. *J Exp Zool* 297A: 52–63, 2003.
12. **Choe KP, Morrison-Shetlar AI, Wall BP, and Claiborne JB.** Immunological detection of Na^+/H^+ exchangers in the gills of a hagfish, *Myxine glutinosa*, an elasmobranch, *Raja erinacea*, and a teleost, *Fundulus heteroclitus*. *Comp Biochem Physiol* 131A: 375–385, 2002.
13. **Choe KP, O'Brien S, Evans DH, Toop T, and Edwards SL.** Immunolocalization of Na^+/K^+-ATPase, carbonic anhydrase II, and, vacuolar H^+-ATPase in the gills of freshwater adult lampreys, *Geotria australis*. *J Exp Zool* 301A: 654–665, 2004.
14. **Choe KP, Verlander JW, Wingo CS, and Evans DH.** A putative H^+/K^+-ATPase in the Atlantic stingray, *Dasyatis sabina*: primary se-

quence and expression in gills. *Am J Physiol Regul Integr Comp Physiol* 287: R981–R991, 2004.
15. **Claiborne JB.** Acid-base regulation. In: *The Physiology of Fishes* (2nd ed.), edited by Evans DH. Boca Raton, FL: CRC, 1998, p. 177–198.
16. **Claiborne JB, Edwards SL, and Morrison-Shetlar AI.** Acid-base regulation in fishes: cellular and molecular mechanisms. *J Exp Zool* 293: 302–319, 2002.
17. **Coates MI and Sequeira SEK.** Early sharks and primitive gnathostome interrelationships. In: *Major Events in Early Vertebrate Evolution*, edited by Ahlberg PE. London: Taylor and Francis, 2001, p. 241–262.
18. **Collins JF, Honda T, Knobel S, Bulus NM, Conary J, Dubois R, and Ghishan FK.** Molecular cloning, sequencing, tissue distribution, and functional expression of a Na^+/H^+ exchanger (NHE-2). *Proc Natl Acad Sci USA* 90: 3938–3942, 1993.
19. **Dyck JRB, Silva NLCL, and Fliegel L.** Activation of the Na^+/H^+ exchanger gene by the transcription factor AP-2. *J Biol Chem* 270: 1375–1381, 1995.
20. **Bendtsen JD, Nielsen H, von Heijne G, and Brunak S.** Improved prediction of signal peptides: SignalP 3.0. *J Mol Biol* 340: 783–795, 2004.
21. **Edwards SL, Donald JA, Toop T, Donowitz M, and Tse CM.** Immunolocalization of sodium/proton exchanger-like proteins in the gills of elasmobranchs. *Comp Biochem Physiol A Mol Integr Physiol* 131: 257–265, 2002.
22. **Edwards SL, Tse CM, and Toop T.** Immunolocalization of NHE3-like immunoreactivity in the gills of the rainbow trout (*Oncorhynchus mykiss*) and the blue-throated wrasse (*Pseudolabrus tetrious*). *J Anat* 195: 465–469, 1999.
23. **Evans DH, Kormanik GA, and Krasny EJ.** Mechanisms of ammonia and acid extrusion by the little skate, *Raja erinacea*. *J Exp Zool* 208: 431–437, 1979.
24. **Evans DH, More KJ, and Robbins SL.** Modes of ammonia transport across the gill epithelium of the marine teleost fish, *Opsanus beta*. *J Exp Biol* 144: 339–356, 1989.
25. **Evans DH, Piermarini PM, and Choe KP.** Homeostasis: osmoregulation, pH regulation, and nitrogen excretion. In: *Biology and Ecology of Sharks and Their Relatives*, edited by Carrier JC. Baca Raton, FL: CRC, 2004, p. 247–268.
26. **Evans DH, Piermarini PM, and Choe KP.** The multifunctional fish gill: dominant site of gas exchange, osmoregulation, acid-base regulation, and excretion of nitrogenous waste. *Physiol Rev* 85: 97–177, 2005.
27. **Gluck S, Underhill D, Iyori M, Holliday S, Kostrominova T, and Lee B.** Physiology and biochemistry of kidney vacuolar H^+-ATPase. *Annu Rev Physiol* 58: 427–445, 1996.
28. **Hayashi H, Szaszi K, and Ginstein S.** Multiple modes of regulation of Na^+/H^+ exchangers. *Ann NY Acad Sci* 976: 248–258, 2002.
29. **Hirata T, Kaneko T, Ono T, Nakazato T, Furukawa N, Hasegawa S, Wakabayashi S, Shigekawa M, Chang MH, Romero M, and Hirose S.** Mechanism of acid adaptation of a fish living in a pH 3.5 lake. *Am J Physiol Regul Integr Comp Physiol* 284: R1199–R1212, 2003.
30. **Hoogerwerf WA, Tsao SC, Devuyst O, Levine SA, Yun CH, Yip JW, Cohen ME, Wilson PD, Lazenby AJ, Tse CM, and Donowitz M.** NHE2 and NHE3 are human and rabbit intestinal brush-border proteins. *Am J Physiol Gastrointest Liver Physiol* 270: G29–G41, 1996.
31. **Johnson MR and Snelson FF.** Reproductive life history of the Atlantic stingray, *Dasyatis sabina* (Pisces, Dasyatidae), in the freshwater St. John's River, Florida. *Bull Mar Sci* 59: 74–88, 1996.
32. **Kandasamy RA and Orlowski J.** Genomic organization and glucocorticoid transcriptional activation of the rat Na^+/H^+ exchanger Nhe3 gene. *J Biol Chem* 271: 10551–10559, 1996.
33. **Katoh F, Hyodo S, and Kaneko T.** Vacuolar-type proton pump in the basolateral plasma membrane energizes ion uptake in branchial mitochondria-rich cells of killifish *Fundulus heteroclitus*, adapted to a low ion environment. *J Exp Biol* 206: 793–803, 2003.
34. **Kumar S, Tamura K, Jakobsen IB, and Nei M.** MEGA2: molecular evolutionary genetics analysis software. *Bioinformatics* 17: 1244–1245, 2001.
35. **Laemmli UK.** Cleavage of structural proteins during the assembly of the head of bacteriophage T4. *Nature* 227: 680–685, 1970.
36. **Ledoussal C, Lorenz JN, Nieman ML, Soleimani M, Schultheis PJ, and Shull GE.** Renal salt wasting in mice lacking NHE3 Na^+/H^+ exchanger but not mice lacking NHE2. *Am J Physiol Renal Physiol* 281: F718–F727, 2001.
37. **Levine SA, Hentrose MH, Tse CM, and Donowitz M.** Kinetics and regulation of three cloned mammalian Na^+/H^+ exchangers stably expressed in a fibroblast cell line. *J Biol Chem* 268: 25527–25535, 1993.
38. **Lin H, Pfeiffer DC, Vogl AW, Pan J, and Randall DJ.** Immunolocalization of H^+-ATPase in the gill epithelia of rainbow trout. *J Exp Biol* 195: 169–183, 1994.
39. **Lin H and Randall DJ.** Proton pumps in fish gills. In: *Cellular and Molecular Approaches to Fish Ionic Regulation*, edited by Wood C and Shuttleworth T. San Diego, CA: Academic, 1995, p. 229–256.
40. **Marshall WS.** Na^+, Cl^-, Ca^{2+}, Zn^{2+} transport by fish gills: retrospective review and prospective synthesis. *J Exp Zool* 293: 264–283, 2002.
41. **Moe OW.** Acute regulation of proximal tubule apical membrane Na/H exchanger NHE-3: role of phosphorylation, protein trafficking, and regulatory factors. *J Am Soc Nephrol* 10: 2412–2425, 1999.
42. **Nei M and Kumar S.** *Molecular Evolution and Phylogenetics*. New York: Oxford University Press, 2000.
43. **Nelson JS.** *Fishes of the World*. New York: Wiley, 1994.
44. **Nelson N and Harvey W.** Vacuolar and plasma membrane proton-adenosinetriphosphatases. *Physiol Rev* 79: 362–379, 1999.
45. **Newman PR, Greeb J, Keeton TP, Reyes AA, and Shull GE.** Structure of the human gastric H,K-ATPase gene and comparison of the 5′-flanking sequences of the human and rat genes. *DNA Cell Biol* 9: 749–762, 1990.
46. **Orlowski J and Grinstein S.** Diversity of the mammalian sodium/proton exchanger SLC9 gene family. *Pflügers Arch* 447: 549–565, 2004.
47. **Orlowski J and Grinstein S.** Na^+/H^+ exchangers in mammalian cells. *J Biol Chem* 272: 22373–22376, 1997.
48. **Orlowski J, Kandasamy RA, and Shull GE.** Molecular cloning of putative members of the NHE exchanger gene family. cDNA cloning, deduced amino acid sequence, and mRNA tissue expression of the rat NHE exchanger NHE-1 and two structurally related proteins. *J Biol Chem* 267: 9331–9339, 1992.
49. **Perry S and Fryer JN.** Proton pumps in the fish gill and kidney. *Fish Physiol Biochem* 17: 363–369, 1997.
50. **Piermarini PM and Evans DH.** Effects of environmental salinity on Na^+/K^+-ATPase in the gills and rectal gland of a euryhaline elasmobranch (*Dasyatis sabina*). *J Exp Biol* 203: 2957–2966, 2000.
51. **Piermarini PM and Evans DH.** Immunochemical analysis of the vacuolar proton-ATPase B-subunit in the gills of a euryhaline stingray (*Dasyatis sabina*): effects of salinity and relation to Na^+/K^+-ATPase. *J Exp Biol* 204: 3251–3259, 2001.
52. **Piermarini PM and Evans DH.** Osmoregulation of the Atlantic stingray (*Dasyatis sabina*) from the freshwater lake Jesup of the St. John's River, Florida. *Physiol Zool* 71: 553–560, 1998.
53. **Piermarini PM, Verlander JW, Royaux IE, and Evans DH.** Pendrin immunoreactivity in the gill epithelium of a euryhaline elasmobranch. *Am J Physiol Regul Integr Comp Physiol* 283: R983–R992, 2002.
54. **Romero MF, Fong P, Berger UV, Hediger MA, and Boron WF.** Cloning and functional expression of rNBC, an electrogenic Na^+-HCO_3^- cotransporter from rat kidney. *Am J Physiol Renal Physiol* 274: F425–F432, 1998.
55. **Royaux IE, Wall SM, Karniski LP, Everette LA, Suzuki K, Knepper MA, and Green ED.** Pendrin, encoded by the Pendred syndrome gene, resides in the apical region of renal intercalated cells and mediates bicarbonate secretion. *Proc Natl Acad Sci USA* 98: 4221–4226, 2001.
56. **Sardet C, Franchi A, and Pouyssegur J.** Molecular cloning, primary structure and expression of the human growth factor-activatable Na^+/H^+ antiporter. *Cell* 56: 271–280, 1989.
57. **Sciortino CM, Shrode LD, Fletcher BR, Harte PJ, and Romero MF.** Localization of endogenous and recombinant Na^+-driven anion exchanger protein NDAE1 from *Drosophila melanogaster*. *Am J Physiol Cell Physiol* 281: C449–C463, 2001.
58. **Stahlberg A, Hakansson J, Xian X, Semb H, and Kubista M.** Properties of the reverse transcription reaction in mRNA quantification. *Clin Chem* 50: 509–515, 2004.
59. **Sullivan GV, Fryer JN, and Perry SF.** Immunolocalization of proton pumps (H^+-ATPase) in pavement cells of rainbow trout gill. *J Exp Biol* 198: 2619–2629, 1995.
60. **Tresguerres M, Katoh F, Fenton H, Jasinska E, and Goss GG.** Regulation of branchial V-H^+-ATPase, Na^+/K^+-ATPase and NHE2 in response to acid and base infusions in the Pacific spiny dogfish (*Squalus acanthias*). *J Exp Biol* 208: 345–354, 2005.
61. **Tse CM, Levine SA, Yun CH, Brant SR, Pouyssegur J, and Donowitz M.** Cloning and sequencing a rabbit cDNA encoding an intestinal and

kidney-specific Na^+/H^+ exchanger isoform (NHE-3). *J Biol Chem* 267: 9340–9346, 1992.
62. **Tse CM, Levine SA, Yun CHC, Montrose MH, Little PJ, Pouysseger J, and Donowitz M.** Cloning and expression of a rabbit cDNA encoding a serum-activated ethylisopropylamiloride-resistant epithelial Na^+/H^+ exchanger isoform (NHE2). *J Biol Chem* 268: 11917–11924, 1993.
63. **Vallon V, Schwark JR, Richter K, and Hropot M.** Role of Na+/H+ exchanger NHE3 in nephron function: micropuncture studies with S3226, an inhibitor of NHE3. *Am J Physiol Renal Physiol* 278: F375–F379, 2000.
64. **Wakabayashi S, Shigekawa M, and Pouyssegur J.** Molecular physiology of vertebrate Na^+/H^+ exchangers. *Physiol Rev* 77: 51–75, 1997.
65. **Wang T, Hropot M, Aronson PS, and Giebisch G.** Role of NHE isoforms in mediating bicarbonate reabsorption along the nephron. *Am J Physiol Renal Physiol* 281: F1117–F1122, 2001.
66. **Wilson J, Morgan J, Vogl W, and Randall D.** Branchial mitochondria-rich cells in the dogfish *Squalus acanthias*. *Comp Biochem Physiol A Mol Integr Physiol* 132: 365–374, 2002.
67. **Wilson J, Randall D, Donowitz M, Vogl W, and Ip A.** Immunolocalization of ion-transport proteins to branchial epithelium mitochondria-rich cells in the mudskipper (*Periophthalmodon schlosseri*). *J Exp Biol* 203: 2297–2310, 2000.
68. **Wilson JM, Laurent P, Tufts BL, Benos DJ, Donowitz M, Vogl AW, and Randall DJ.** NaCl uptake by the branchial epithelium in freshwater teleost fish: an immunological approach to ion-transport protein localization. *J Exp Biol* 203: 2279–2296, 2000.
69. **Wilson JM, Whiteley NM, and Randall DJ.** Ionoregulatory changes in the gill epithelia of coho salmon during seawater acclimation. *Physiol Biochem Zool* 75: 237–249, 2002.
70. **Woo AL, Noonan WT, Schultheis PJ, Neumann JC, Manning PA, Lorenz JN, and Shull GE.** Renal function in NHE3-deficient mice with transgenic rescue of small intestine absorptive defect. *Am J Physiol Renal Physiol* 284: F1190–F1198, 2003.
71. **Xie Q, Welch R, Mercado A, Romero MF, and Mount DB.** Molecular characterization of the murine Slc26a6 anion exchanger: functional comparison with Slc26a1. *Am J Physiol Renal Physiol* 283: F826–F838, 2002.
72. **Yun CHC, Lamprecht G, Forster DV, and Sidor A.** NHE3 kinase a regulatory protein E3KARP binds the epithelial brush border Na^+/H^+ exchanger NHE3 and the cytoskeletal protein ezrin. *J Biol Chem* 273: 25856–25863, 1998.
73. **Yun CHC, Tse CM, Nath SK, Levine SA, Brant SR, and Donowitz M.** Mammalian Na^+/H^+ exchanger gene family: Structure and function studies. *Am J Physiol Gastrointest Liver Physiol* 269: G1–G11, 1995.
74. **Zizak M, Cavet ME, Bayle D, Tse CM, Hallen S, Sachs G, and Donowitz M.** Na^+/H^+-Exchanger NHE3 has 11 membrane spanning domains and a cleaved signal peptide: topology analysis using in vitro transcription/translation. *Biochemistry* 39: 8102–8112, 2000.